PHYSICAL REVIEW A **77**, 041802(R) (2008)

Image storage in hot vapors

L. Zhao,[1] T. Wang,[1] Y. Xiao,[2] and S. F. Yelin[1,3]
[1]*Department of Physics, University of Connecticut, Storrs, Connecticut 06269, USA*
[2]*Harvard-Smithsonian Center for Astrophysics, Cambridge, Massachusetts 02138, USA*
[3]*ITAMP, Harvard-Smithsonian Center for Astrophysics, Cambridge, Massachusetts 02138, USA*
(Received 9 October 2007; published 10 April 2008)

We theoretically investigate image storage in hot atomic vapor. A so-called $4f$ system is adopted for imaging and an atomic vapor cell is placed over the transform plane. The Fraunhofer diffraction pattern of an object in the object plane can thus be transformed into atomic Raman coherence according to the idea of "light storage." We investigate how the stored diffraction pattern evolves under diffusion and discuss the essence of the stability of its dark spots. Our result indicates, under appropriate conditions, that an image can be reconstructed with high fidelity. The main reason for this procedure is the fact that diffusion of opposite-phase components of the diffraction pattern interferes destructively.

DOI: 10.1103/PhysRevA.77.041802 PACS number(s): 42.30.−d, 42.50.Gy

Manipulating images all optically may play a significant role in many fields, including holography, remote sensing, classic or quantum correlations, image and information processing, etc. In many applications, the amplitude and phase of images should be preserved. Recently, some studies of the propagation and storage of images were performed [1–4]. Electromagnetically induced transparency (EIT), a phenomenon of quantum interference, has been investigated for decades [5–7]. In the EIT system, the propagation of light fields can be described by coupled light-matter excitations termed "dark-state polariton." The weak probe light can be manipulated coherently and all optically, and its amplitude and phase can be preserved [8–12]. Hence, an EIT system may be a good candidate for manipulating images [13].

For experiments based on EIT mostly hot atomic vapor cells are adopted because of ease of use and fabrication [14,15]. The Raman coherence, however, carried by the atoms will diffuse due to the atomic motion [16,17]. Thus, the transverse distortion induced by diffusion could pose a real challenge to processing images, especially small ones.

In this paper, we theoretically demonstrate that, similar to the storage of optical vortices [17], the dark spots of the Fraunhofer diffraction pattern of an object in a $4f$ imaging system can be stored for a long time under strong diffusion conditions. The essence of such stability depends on the destructive interference of the coherence. Furthermore, using the principle of Fourier optics [18], the spatial information of the object can be mapped into the diffraction pattern. Under appropriate conditions, an image with high fidelity can form on the screen in the presence of diffusion. In contrast to the recent image storage [4], our scheme is free from the artificial "phase-shift lithography" technique [19], where, for an unknown arbitrary image, it might be difficult to make the corresponding phase plate beforehand.

A $4f$ imaging system is shown in Fig. 1(a), which consists of two identical lenses with focal length f. An object is put in the front focal plane (X_O, Y_O) of the first lens and the image can be retrieved in the back focal plane (X_I, Y_I) of the second lens. The distance between the two lenses is $2f$. The back focal plane of the first lens coincides with the front focal plane of the second lens, and is called the "transform plane" (TP) with coordinates (X, Y). The optical axes of the two lenses coincide, and are defined as the "Z" axis. According to the Abbe theory [18], the Fraunhofer diffraction pattern of the object is produced near the TP. To store the pattern, a short vapor cell is placed over this plane. In the cell, the EIT medium can be described as a three-level Λ system with both the pattern and coupling lights resonant with the respective optical transition $1 \leftrightarrow 2$, or $1 \leftrightarrow 3$ [Fig. 1(c)].

To illustrate how the stored diffraction pattern evolves, we discuss the simplest case in which the object is a single slit of width a centered around the Z axis. It is uniformly illuminated by a normally incident weak pulse with central wavelength λ, whose spectral width lies within the EIT window generated by the coupling light. The complex amplitude of the Fraunhofer diffraction pattern of the single slit can be written

$$E_{12}^{(1)}(x) = C\,\mathrm{sinc}(\alpha x), \tag{1}$$

where C is a constant, and $\alpha = \pi a/(f\lambda)$ is the transverse wave number. Because the length of the cell s is much smaller than the focal length ($s \ll f$), the distance between the trapped pat-

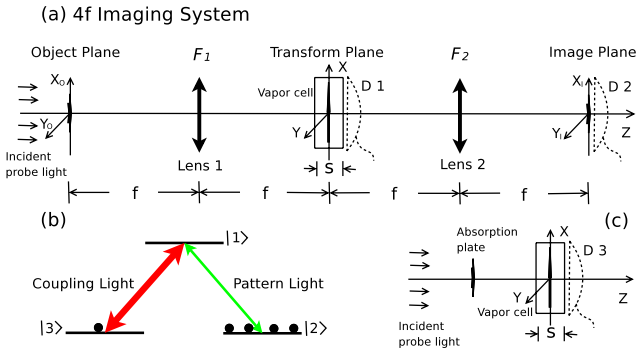

FIG. 1. (Color online) (a) $4f$ imaging system. F_1/F_2 means a Fourier transform through lens 1/2. D1/D2 can measure the retrieved diffraction pattern/image. (b) The three-level Λ system coupled with the pattern and coupling lights. (c) A diagram for the storage of an "artificial pattern" in the near-field zone. D3 can measure the retrieved artificial pattern. D: Detector. In (a) and (c), the copropagating coupling beams and some beamsplitters are omitted.

tern and the first lens d is very close to f. Thus, we ignore the quadratic phase factor $\exp[i\frac{\pi}{\lambda f}(1-\frac{f}{d})x^2]$. The sinc pattern of Eq. (1) has many zero crossings, i.e., dark spots. Two of them are at $\alpha x = \pm\pi$, and the parts on both sides of the dark spots along the X axis have a π phase shift.

For comparison, we also investigate an artificial pattern which has two dark spots at $\alpha x = \pm\pi$ as well, but the parts on both sides of the dark spots along the X axis are in phase with each other. The artificial pattern can be produced by passing a pulse through an absorption plate. In the near-field zone after the plate [Fig. 1(c)], its complex amplitude could be given by

$$E_{12}^{(2)}(x) = C\left(\cos\frac{\alpha x}{2}\right)^2 \exp\left(-\frac{x^2}{w^2}\right), \tag{2}$$

where w is the width of the pulse. In what follows, we can see how the difference between the patterns affects the existence of dark spots.

After the coupling lights are switched off, the Raman coherence, described by the off-diagonal density matrix element ρ_{23}, in the hot vapor is given by [9]

$$\rho_{23}(x,t=0) = -\frac{g}{\Omega_{13}} E_{12}^{(1,2)}(x), \tag{3}$$

where g is the atom-field coupling constant, Ω_{13} is the Rabi frequency of the strong coupling light before it is turned off, $t=0$ means Eq. (3) is the initial condition of the diffusion process, which then is described by

$$\frac{\partial \rho_{23}(x,t)}{\partial t} = D\frac{\partial^2 \rho_{23}(x,t)}{\partial x^2}, \tag{4}$$

where D is the diffusion coefficient. In fact, in our scheme, the diffusion of ρ_{23} in the (X,Y) plane is independent of the propagation of the pattern in the Z direction. Hence, Eq. (4) not only describes the diffusion of the stored pattern, but also describes that of the slowed one. To solve Eq. (4), we introduce the one-dimensional (1D) diffusion propagator $G(x,x',t)=(4\pi Dt)^{-1/2}\exp(-(x-x')^2/4Dt)$ [4,17], yielding

$$\rho_{23}(x,t) = \int_{-\infty}^{+\infty} \rho_{23}(x',t=0)G(x,x',t)dx'. \tag{5}$$

We can quantitatively compare the time evolution of the stored Raman coherence of both patterns in Fig. 2. Initially, both patterns have dark spots at $\alpha x = \pm\pi$. When the diffusion begins, the dark spots of the artificial pattern will disappear quickly, but those of the diffraction pattern can exist for much longer and only slightly move outward. The outward motion of the dark spots in both patterns comes from the coherence gradient of ρ_{23}. For the diffraction pattern which has a 1D spatial phase structure, when the out-of-phase parts diffuse into the dark spots in the opposite directions, the destructive interference will occur, and the dark spots will remain. For the artificial pattern, however, everything is *in* phase, no destructive interference occurs, and the dark spots will be filled in right when the diffusion begins.

Generally, the existence of dark spots in the Fraunhofer diffraction pattern can be described in terms of the destructive interference of dark-state polaritons. In principle, for some higher electromagnetic modes, such as $HG_{1,1}$ (Hermite-Gaussian) with a two-dimensional (2D) spatial phase structure, the dark centers and lines can also be stored stably even without moving, which is due to both the destructive interference and the geometric symmetry of the phase structures. In fact, a stored optical vortex [17] is just a special example.

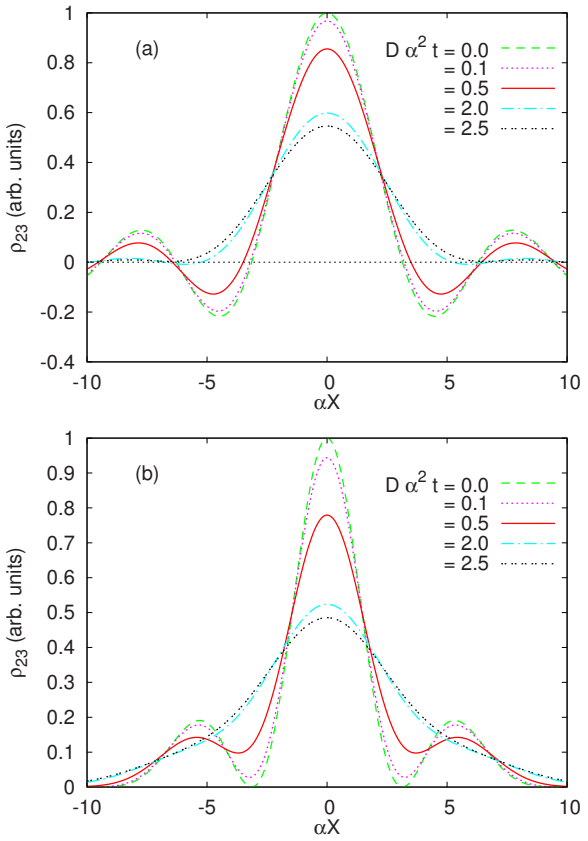

FIG. 2. (Color online) (a) The diffusion of the diffraction pattern. The dark spots will exist for a long time and move outward. (b) The diffusion of the artificial pattern. The dark spots will disappear very quickly after the diffusion begins. Parameters are $f=25$ cm, $\lambda=795$ nm, $a=100$ μm, $w=\sqrt{20}/\alpha$. From the above graphs, we can see the dark spots of diffraction pattern still exist even when $D\alpha^2 t=2$. From [16], when $D=1.5$ cm$^2/s$ (weak diffusion), $t\approx 5336.5$ μs; when $D=30$ cm^2/s (strong diffusion), $t\approx 266.8$ μs. These results show dark spots of the diffraction pattern are robust to the diffusion of atoms. All the parameters are not optimized.

One more point should be noted. We have only investigated the diffusion of Raman coherence (ρ_{23}) and seen the long-term existence of dark spots. In contrast, the atomic populations (ρ_{22},ρ_{33}) are diffusing *without* interference. This can lead to fluorescence emitted in all directions in the retrieval process [20]. In our probe direction [the positive Z direction in Fig. 1(a)], however, the fluorescence is very weak compared with the retrieved diffraction pattern, and will not seriously change the visibility. Thus, this effect can be neglected in our case.

Next, we consider image formation in the image plane (IP) of Fig. 1(a). The above single slit in the $4f$ imaging

system can be replaced by an actual 2D object. The complex amplitude of the outgoing wave right after the object is $E_O(x_O,y_O)$. Through lens 1 the diffraction pattern in the TP can be expressed as $E(x,y)=F_1[E_O(x_O,y_O)]$. While being trapped, the 2D diffraction pattern will be transformed into the Raman coherence, whose motion can be described by the 2D diffusion equation

$$\frac{\partial \rho_{23}(x,y,t)}{\partial t} = D\left(\frac{\partial^2}{\partial x^2} + \frac{\partial^2}{\partial y^2}\right)\rho_{23}(x,y,t). \quad (6)$$

Similar to Eq. (3), $\rho_{23}(x,y,t)$ can be expressed through $E(x,y,t)$.

In order to solve Eq. (6), the Fourier transform is performed in the TP, which is seen to be $F_2[E(x,y,t)]$. Note that this expression is already the electric field in the IP $E_I(x_I,y_I,t)$. For the initial condition, the Fourier transform is $F_2[E(x,y,t=0)]=E_I(x_I,y_I,t=0)$.

The diffusion Eq. (6) with the initial condition becomes

$$\frac{d}{dt}E_I(x_I,y_I,t) + \beta E_I(x_I,y_I,t) = 0,$$

where

$$E_I(x_I,y_I,t=0) = F_2[F_1[E_O(x_O,y_O)]]$$

and

$$\beta = D(2\pi)^2(x_I^2 + y_I^2)/\lambda^2 f^2. \quad (7)$$

This equation is the time-evolution equation of the image we are interested in. The solution of Eq. (7) is

$$E_I(x_I,y_I,t) = E_O(-x_I,-y_I)\exp(-\beta t). \quad (8)$$

Equation (8) teaches us four features of the image: (i) the image is inverted with respect to the object, (ii) the phase of the image is preserved, (iii) the amplitude at the edges of the image will decay faster than that at the center, and (iv) the dark part of the image is always dark and therefore the borders are always sharp. [The intensity is given by $I_I(x_I,y_I,t) \propto |E_I(x_I,y_I,t)|^2$.]

To quantitatively characterize the evolution of images due to diffusion, we define the fidelity by

$$FI(t) = |\langle \Psi(x_I,y_I,t=0)|\Psi(x_I,y_I,t)\rangle|^2, \quad (9)$$

with

$$\Psi(x_I,y_I,t=0) = \frac{E_I(x_I,y_I,t=0)}{\sqrt{\int\int |E_I(x_I,y_I,t=0)|^2 dx_I dy_I}}, \quad (10)$$

$$\Psi(x_I,y_I,t) = \Psi(x_I,y_I,t=0)\exp(-\beta t), \quad (11)$$

where Eq. (10) is the normalized initial wave function, and Eq. (11) is the time-evolving wave function. For comparison, we also analyze the direct storage of images (e.g., the vapor cell is placed over the IP in Fig. 1(a), similar to the setup in Ref. [4]). The retrieved wave function is

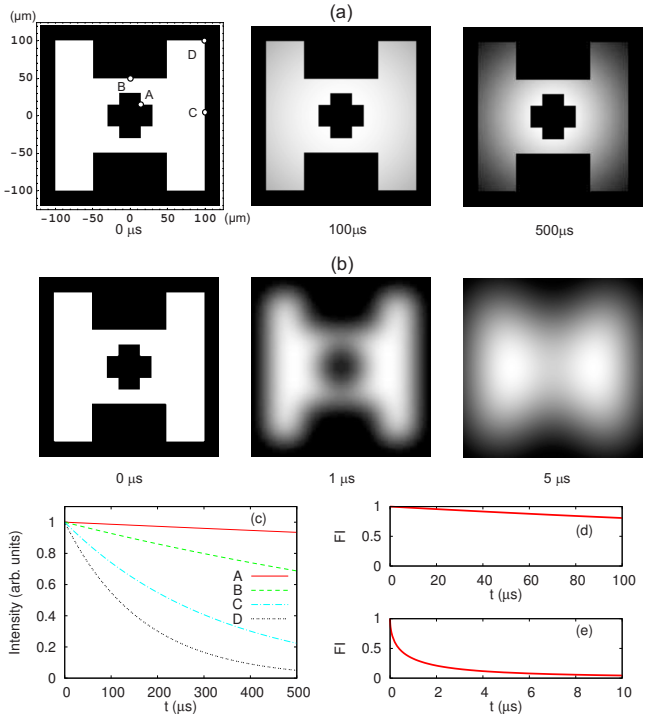

FIG. 3. (Color online) The object is centered on the Z axis, and has a letter "H" with a dark cross at the center. The coordinates of points A, B, C, D are (15,15), (0,50), (100,0), (100,100) in μm, respectively. Parameters are $D=1.5\ \mathrm{cm}^2/\mathrm{s}$, $f=25$ cm, and $\lambda=795$ nm. (a) The time evolution of the image stored in the TP and (b) in the IP. (c) The intensities at different points in (a) varying with time. (d) The fidelity of the whole image stored in the TP varying with time, and (e) in the IP. All the parameters are not optimized. Note the different time scales in (a) and (b), (d) and (e).

$$\Psi(x_I,y_I,t) = \int\int_{-\infty}^{+\infty} \Psi(x_I,y_I,t=0)G(x_I,x_I',y_I,y_I',t)dx_I'dy_I', \quad (12)$$

where $G(x_I,x_I',y_I,y_I',t)=(4\pi Dt)^{-1}\exp[(-(x_I-x_I')^2-(y_I-y_I')^2)/4Dt]$ is the 2D diffusion propagator [4,17].

As an example, Fig. 3 shows the storage of the image of a letter "H" with a dark cross at the center. From Fig. 3(a), we can see two aforementioned features explicitly: (i) the binary edges of the bright image do not move, but the intensity at the edges does decrease. However, as long as the weakest intensity [e.g. the intensity at point D at the corner see Fig. 3(c)] is higher than the threshold of the detector, the edges of the image are still detectable, and the shape of the image is preserved; (ii) the dark part is always dark. To explain (ii), let us consider the simplest case, in which a dark wire in the object plane is illuminated by a plane wave. According to Babinet's principle [21], in the TP, the diffraction pattern of the dark wire is a bright spot (the diffraction pattern of the plane wave is, mathematically, a delta function) superimposed on the diffraction pattern of a single slit (the complementary object of the dark wire). Because the diffusion equation is linear, both diffraction patterns will diffuse synchronically. This can lead to the fact that the amplitude at

the image of the dark wire in the IP will always exactly cancel out and the dark part keeps dark. In fact, this phenomenon can be considered as a result of destructive interference between two diffused diffraction patterns. In contrast, in Fig. 3(b), because no destructive interference occurs, the whole image gets blurred very quickly.

Finally, we will provide some estimates of potential experimental setups. First, the aberrations of the spherical lens may cause a problem [22]. To estimate this effect, we consider an actual lens with the radii of surface curvature $R_1 = -R_2 = 25$ cm, the thickness at the center $d = 4$ mm, and the refractive index $n = 1.5$, thus, the effective focal length $1/f = (n-1)(1/R_1 - 1/R_2 + (n-1)d/nR_1R_2) \approx 1/25$ cm. Given a beam with the radius of 1 cm centered around and parallel to the Z axis, one can calculate directly with Snell's law [22] and find the difference between the focal length of the marginal rays and that of the central rays is only about 1 mm, which is much smaller than $f \approx 25$ cm. This means the aberrations are very small and could not seriously affect the phase structure of the diffraction pattern and the Fourier transform is well defined in our system. Moreover, we can use a parabolic lens system to minimize the aberrations. Second, the angular deviation between the pattern light and the coupling light is unavoidable, which induces the *residual* Doppler shift in hot vapors and lowers the storage efficiency [23]. In our case, given the coupling light in the Z direction, according to the Huygens-Fresnel principle [22], the maximum misalignment in the TP comes from the spherical secondary wavelets emitted at the corners [e.g., point D in Fig. 3(a)], which has the angular deviation of $\approx 5.7 \times 10^{-4}$ rad with respect to the Z axis. Additionally, the Dicke-like narrowing effect induced by the buffer gas collisions can strongly suppress the residual Doppler broadening [24,25]. Thus, our storage process is robust.

In summary, we have shown that the stored dark spots of the Fraunhofer diffraction pattern in a $4f$ imaging system can exist for a long time under strong diffusion. Unlike in Ref. [17], the essence of such stability depends only on the destructive interference of atomic coherence, is independent of geometric dimensionality and topological nature, and originates from the spatial coherence of dark-state polaritons. Furthermore, we discussed the influence of diffusion of the coherence on imaging and found that our scheme can dramatically enhance the stability of a stored image in hot vapors [26]. In principle, this discussion could be applied to other coherent slow light or light storage processes for imaging in the media with diffusion, such as [1]. Although the storage of Fraunhofer diffraction pattern discussed above is a classic process, it can also go to a few photon regime, which may have interesting applications in quantum image storage, or buffering and processing associated with Fourier optics.

We would like to acknowledge funding from the NSF. L. Z. thanks A. Kovner and R. Zhou for discussions.

[1] R. M. Camacho, C. J. Broadbent, I. Ali-Khan, and J. C. Howell, Phys. Rev. Lett. **98**, 043902 (2007).
[2] A. Kasapi, M. Jain, G. Y. Yin, and S. E. Harris, Phys. Rev. Lett. **74**, 2447 (1995).
[3] M. Jain, A. J. Merriam, A. Kasapi, G. Y. Yin, and S. E. Harris, Phys. Rev. Lett. **75**, 4385 (1995).
[4] M. Shuker, O. Firstenberg, R. Pugatch, A. Ron, and N. Davidson, eprint arXiv:quant-ph/0707.3707.
[5] S. E. Harris, Phys. Today **50**(7), 36 (1997).
[6] M. D. Lukin, Rev. Mod. Phys. **75**, 457 (2003).
[7] M. Fleischhauer, A. Imamoglu, and J. P. Marangos, Rev. Mod. Phys. **77**, 633 (2005).
[8] L. V. Hau, S. E. Harris, Z. Dutton, and C. H. Behroozi, Nature (London) **397**, 594 (1999).
[9] M. Fleischhauer and M. D. Lukin, Phys. Rev. Lett. **84**, 5094 (2000).
[10] M. Fleischhauer and M. D. Lukin, Phys. Rev. A **65**, 022314 (2002).
[11] C. Liu, Z. Dutton, C. H. Behroozi, and L. V. Hau, Nature (London) **409**, 490 (2001).
[12] A. V. Turukhin, V. S. Sudarshanam, M. S. Shahriar, J. A. Musser, B. S. Ham, and P. R. Hemmer, Phys. Rev. Lett. **88**, 023602 (2001).
[13] A. L. Gaeta, Nat. Photonics **1**, 140 (2007).
[14] D. F. Phillips, A. Fleischhauer, A. Mair, R. L. Walsworth, and M. D. Lukin, Phys. Rev. Lett. **86**, 783 (2001).
[15] M. Bajcsy, A. S. Zibrov, and M. D. Lukin, Nature (London) **426**, 638 (2003).
[16] Y. Xiao, I. Novikova, D. F. Phillips, and R. L. Walsworth, Phys. Rev. Lett. **96**, 043601 (2006).
[17] R. Pugatch, M. Shuker, O. Firstenberg, A. Ron, and N. Davidson, Phys. Rev. Lett. **98**, 203601 (2007).
[18] J. W. Goodman, *Introduction to Fourier Optics*, 2nd ed. (McGraw-Hill, New York, 1996).
[19] M. D. Levenson, Phys. Today **46**(7), 28 (1993).
[20] T. Wang, L. Zhao, L. Jiang, and S. F. Yelin, Phys. Rev. A **77**, 043815 (2008).
[21] M. Babinet, C. R. Hebd. Seances Acad. Sci. **4**, 638 (1837).
[22] E. Hecht, *Optics*, 2nd ed. (Addison-Wesley, Massachusetts, 1987) (reprinted in 1990).
[23] P. R. S. Carvalho, L. E. E. de Araujo, and J. W. R. Tabosa, Phys. Rev. A **70**, 063818 (2004).
[24] O. Firstenberg, M. Shuker, A. Ben-Kish, D. R. Fredkin, N. Davidson, and A. Ron, Phys. Rev. A **76**, 013818 (2007).
[25] M. Shuker, O. Firstenberg, R. Pugatch, A. Ben-Kish, A. Ron, and N. Davidson, Phys. Rev. A **76**, 023813 (2007).
[26] This method with the destructive phase coherence works well only for black and white and not gray scale contrast.